



# Effect of stitching on the static and fatigue properties of fibre-dominated and matrix-dominated composite laminates

G. Loi, F. Aymerich\*

Department of Mechanical, Chemical and Materials Engineering, University of Cagliari, Italy

## ARTICLE INFO

### Keywords:

A. 3-Dimensional reinforcement  
B. Fatigue  
E. Stitching  
Damage

## ABSTRACT

The paper reports the results of an experimental investigation into the effect of stitching on the static and fatigue response of fibre-dominated and matrix-dominated laminates. The tests were conducted on stitched carbon/epoxy laminates with quasi-isotropic  $[0/\pm 45/90]_s$  or angle-ply  $[+30_2/-30_2]_s$ ,  $[+45_2/-45_2]_s$ ,  $[+60_2/-60_2]_s$  layups. The analyses show that stitching significantly reduces both the static and the fatigue strength of fibre-dominated  $[0/\pm 45/90]_s$  laminates, owing to the presence of localized fibre damage introduced during the stitching process. On the other hand, stitching does not affect the fatigue response of  $[+60_2/-60_2]_s$  laminates but significantly improves the fatigue strength of  $[+30_2/-30_2]_s$  and  $[+45_2/-45_2]_s$  laminates. The effectiveness of stitching on the fatigue performance of the angle-ply layups was found to be directly related to the specific damage mechanisms preceding the ultimate failure, which are controlled by edge delaminations in  $[+30_2/-30_2]_s$  and  $[+45_2/-45_2]_s$  and transverse matrix cracking in  $[+60_2/-60_2]_s$  laminates.

## 1. Introduction

Owing to their high specific strength and stiffness, excellent fatigue and corrosion resistance, and superior design flexibility as compared to conventional metallic materials, fibre reinforced composite materials are being increasingly used for structural applications in many industrial areas, ranging from the aerospace and wind energy sectors to the surface and marine transportation fields.

Laminated composite materials provide remarkable in-plane mechanical performances but have comparatively low out-of-plane strength properties, as a direct consequence of the lack of fibrous reinforcement along the thickness direction. The inherent through-thickness weakness of composite laminates is a serious design limitation for this class of materials, since even relatively low peeling or shear interfacial stresses may exceed the strength of the interface, thus promoting the initiation of delaminations between layers. Delaminations may significantly reduce the local stiffness and the strength of the material [1], and various approaches have been therefore proposed in the past decades to improve the delamination resistance of laminated composites. Among these approaches, we may cite the use of high strain fibres or thermoplastic matrices, the enhancement of fibre–matrix adhesion, the optimization of the laminate layup, the insertion of tough films or nanoparticles between plies, the introduction of through-the-thickness

structural reinforcements (stitching, z-pinning, braiding, and weaving) [2–8].

Stitching has proved particularly effective in enhancing the resistance to delamination of composite laminates, since the bridging mechanism developed by stitches across delaminated interfaces restrains opening or sliding displacements of the crack surfaces, thus preventing or delaying the progression of delaminations [9–10]. Stitching was found to significantly improve many properties of composite laminates, such as mode I and mode II fracture resistance (increases in fracture energy of more than 10 times were for example measured under mode I in DCB tests) [11–13], impact damage resistance [14–16], and post impact damage tolerance [17–18].

However, serious deteriorations of the in-plane strength properties are often observed in stitched composites [3,9,10,19], even though the experimental data available in the literature are somewhat conflicting, as both the compressive and the tensile static strengths have been reported as being reduced, unchanged or improved by stitching in different studies [10,20–28].

In comparison with the significant research work carried out on the static behaviour, only a few studies have been conducted to characterize the effect of stitching on the fatigue response of composite laminates. Earlier experimental investigations were mainly concerned with the fatigue resistance under compressive loading, with almost all studies

\* Corresponding author.

E-mail address: [francesco.aymerich@dimcm.unica.it](mailto:francesco.aymerich@dimcm.unica.it) (F. Aymerich).

[21,29–33] reporting fatigue lives shortened or at best unaffected by stitching. Dow and Smith reported in [30] that stitching degraded the fatigue resistance of flat carbon/epoxy coupon specimens, although it did not modify the fatigue lives of open hole notched samples. Comparable fatigue lives of unstitched and stitched uniweave carbon/epoxy laminates were also reported in [21]. Furrow and coworkers [32] examined the effect of Kevlar and glass stitching on the compression-compression fatigue performance of quasi-isotropic carbon/epoxy laminates under different environmental condition. They observed that while Kevlar stitches did not affect the fatigue response of the base laminates, the insertion of glass stitches led to a reduced fatigue strength, which was attributed to the presence of significant micro-cracking introduced around the stitches during the manufacturing process. Herszberg and co-workers [33] characterized the behaviour of open-hole laminates under tension–compression cyclic loading and found that while the fatigue life of high-density stitched samples was shorter than that of unstitched samples, low-density stitched samples had better fatigue resistance than equivalent unstitched samples.

Apart from a few notable exceptions [24,34], it is only more recently that some investigations have been carried out to assess the fatigue properties of stitched composite laminates under tensile loads [25,26,35–38]. A large amount of research has been performed by Mouritz and coworkers to analyse the fatigue performance of laminates with different types of through-thickness reinforcement (stitching, Z-pinning, 3D weaving) [24,26,27,39,40]. In particular, the fatigue response of fibre-dominated woven glass/vinyl-ester laminates stitched by Kevlar yarns and manufactured by resin infusion was extensively studied to clarify the role of stitches in the evolution of the damage mechanisms leading to fatigue failure [24,26,39]. The experiments showed that while stitching did not significantly affect the static tensile strength of the laminates, it significantly degraded their fatigue performance, with fatigue lives of stitched specimens always shorter than those of unstitched counterpart samples. Even though stitched and unstitched samples exhibited analogous damage features (mainly consisting of transverse matrix cracks, fibre matrix debonding and short delaminations), damage growth was faster in stitched laminates, especially in the vicinity of  $0^\circ$  fibres crimped by stitches, which promoted the initiation and propagation of matrix cracks. It was also observed that samples with the stitch rows aligned parallel to the load direction exhibited better fatigue resistance than samples stitched transversely to the load axis; the difference in the fatigue performance was attributed to the larger amount of crimping sustained by the  $0^\circ$  load bearing fibres of transversely stitched laminates as compared to that of laminates stitched along the axial direction. Significant reductions of the tensile fatigue strength, especially at high stress levels, are also reported in [36] for carbon/epoxy laminates made of non-crimped ( $0^\circ/90^\circ$ ) fabrics and stitched with polyester or low-melt thermoplastic yarns. The influence of the sewing direction on the fatigue behaviour was also observed by Carvelli et al. in a study on the tensile fatigue response of carbon/epoxy laminates made of non crimp fabrics [37]. The study showed that the fatigue life of the laminates was reduced when loaded perpendicularly to the stitch rows but improved when loaded parallel to the stitching direction. The damage mechanisms induced by cyclic loads in unstitched and stitched laminates were found to be significantly different, with damage mainly characterized by extensive edge delaminations in unstitched laminates as opposed to matrix cracking in stitched samples.

The fatigue strength and the damage response of Vectran stitched laminates manufactured with uniweave carbon preforms was studied by Yudhanto and coworkers [38], who observed comparable fatigue lives of unstitched and stitched fibre-dominated laminates. Stitches were capable of restraining delamination growth at the specimen edges but promoted the earlier formation of transverse matrix cracks. A comparison of the effect of stitching on the fatigue behaviour of laminates with fibre dominated and matrix dominated layups was carried out in [25] by examining the response of  $[\pm 45/0/90]_s$  and  $[\pm 30/90]_s$  samples made with unidirectional prepreg layers and selectively stitched along the

edges by Kevlar threads. It was found that stitching degraded the fatigue performance of fibre-dominated laminates, but significantly increased the fatigue life of matrix-dominated laminates. The improved fatigue performance of matrix-dominated laminates was attributed to the action of stitches that delay the propagation of edge delaminations. In fibre-dominated  $[\pm 45/0/90]_s$  laminates, in contrast, individual stitches were prone to failure, thereby significantly reducing their effectiveness for restraining delamination growth. Further experimental evidence of the influence of the laminate layup on the efficacy of stitching is reported in [35], where comparable fatigue lives for matrix-dominated laminates, but much shorter fatigue lives for fibre-dominated laminates, are reported after stitching carbon/bismaleimide laminates with Kevlar threads. Similar trends were observed by Mouritz et al. on the fatigue response of fibre-dominated and matrix-dominated carbon/epoxy laminates reinforced with Z-pins [40].

An overall analysis of the literature data on the fatigue of stitched composites indicates that the tensile fatigue strength of laminated composites is mostly reduced or at best unchanged by stitching. The degradation of the tensile fatigue properties is generally attributed to the defects introduced in the material during the stitching process, such as fibre breakage and micro-structural distortion (fibre waviness and crimping, resin rich regions). The stress concentrations produced around the stitches by these defects promote the initiation of matrix damage and accelerate the fatigue damage growth of stitched laminates [9,19]. The large mismatch between the elastic properties of the stitches and the surrounding laminate was also suggested as a likely cause for stitch/resin debonding and subsequent associated matrix damage [10]. A few studies, however, show that increases in fatigue life may indeed be achieved by stitching [25,34] and indicate that the efficacy of stitches is strongly dependent on the layup of the laminate.

In this regard, it should be remarked that most of the data on the fatigue behaviour of stitched laminates have been obtained on fibre-dominated layups, while very little experimental testing has been done on matrix-dominated layups. Angle-ply laminates, in particular, may offer specific advantages over more conventional fibre-dominated layups with regard to various properties of practical interest in structural applications, such as energy absorption, fracture toughness, shear stiffness, manufacturability and formability, etc. [41].

Additional analyses are therefore required to acquire a more comprehensive understanding of the role of stitches in the fatigue response of the two classes of laminates, which exhibit substantial differences in nature and extent of damage modes. With this aim, this study examines and compares the effect of stitching on the tensile properties of fibre-dominated and matrix-dominated laminates. The experimental observations were carried out on quasi-isotropic ( $[(0/\pm 45/90)]_s$ ) and angle-ply ( $[\pm \theta_2/-\theta_2]_s$ , with  $\theta = 30, 45$  and  $60$ ) laminates. These specific angle-ply layups were chosen so as to examine the role of stitches for ultimate failure conditions governed by different key damage mechanisms: edge delaminations in the  $[\pm 30_2/-30_2]_s$  layup, intralaminar matrix cracking in the  $[\pm 60_2/-60_2]_s$  layup, and a combination of them in the  $[\pm 45_2/-45_2]_s$  layup [42]. The analyses were especially focused on exploring the dependence between the key damage modes and the mechanisms by which the stitches control the structural response of the laminate.

## 2. Materials and experimental methods

Composite panels with four different layups were laminated using unidirectional carbon/epoxy prepreg tapes (Seal Texipreg® HS160/REM, with 64% fibre weight fraction). Fibre-dominated ( $[(0/\pm 45/90)]_s$ ) and matrix-dominated ( $[\pm 30_2/-30_2]_s$ ,  $[\pm 45_2/-45_2]_s$ ,  $[\pm 60_2/-60_2]_s$ ) panels were manufactured with the aim of assessing and comparing the effect of stitching in the presence of different damage processes and failure modes. The uncured prepreg laminates were stitched with twisted polyethylene rovings Dyneema® SK65 ( $3 \times 220$  dtex) by an industrial sewing machine using the modified lock stitch [3] shown in

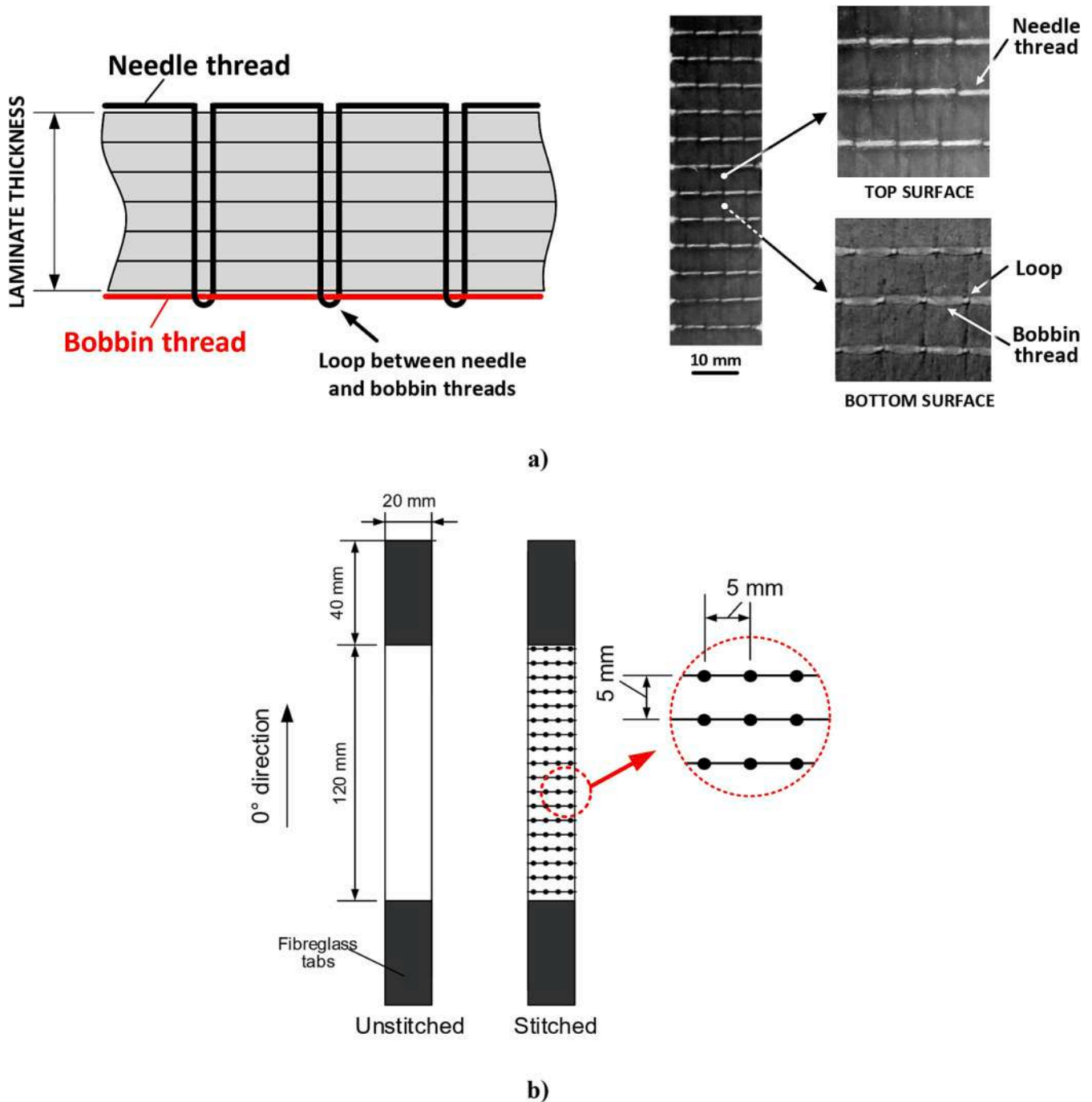


Fig. 1. Modified lock stitch (a) and geometry of samples and stitching pattern (b).

Fig. 1a. In the modified lock stitch, the loop between the needle and the bobbin threads occurs at the bottom surface of the laminate, thus reducing distortion of the fibrous architecture within the laminate. Stitching through prepreg layers typically results in more severe fibre damage than stitching through dry fabrics, since, owing to the high viscosity of the uncured resin, the fibres cannot be easily moved aside by the needle action. To reduce manufacturing fibre damage, the prepreg layers were heated before stitching to reduce resin viscosity and sewing was performed at a low speed (about 60 stitches/min). The panels were stitched perpendicularly to the 0° direction of the laminates (Fig. 1b) and both the stitch step (distance between adjacent stitching rows) and the stitch spacing (distance between successive stitches along a stitching row) were kept at 5 mm. It is worth noting that the density of the

stitching pattern (0.04 stitches/mm<sup>2</sup>) and the linear density of the thread (660 dtex) adopted in this study are within the typical ranges adopted by most of the studies on stitched composites [43]. The main mechanical and thermal properties of the prepreg and thread materials are reported in Table 1. The elastic and strength properties of the unidirectional lamina were obtained by tensile tests on [0]<sub>8</sub> and [+45<sub>2</sub>/−45<sub>2</sub>]<sub>s</sub> laminates, while the elastic properties of the Dyneema fibres and the thermal properties were taken from references [44,45].

After the stitching process was complete, the laminated panels were vacuum bagged and cured in a hydraulic hot press at a pressure of 6 bar and a temperature of 120 °C for 3 h. Unstitched laminates were also laid up and cured under the same conditions as the stitched laminates for use as control materials. No significant difference was observed between the

**Table 1**

Main properties of prepreg material and Dyneema SK65 fibres.

Elastic, strength and thermal [44] properties of the unidirectional prepreg lamina	$E_x = 129$ GPa; $E_y = 8.1$ GPa; $\nu_{xy} = 0.32$ ; $E_s = 4.3$ GPa $X_t = 1750$ MPa; $Y_t = 27$ MPa; $S = 55$ MPa $\alpha_x = -0.3 \times 10^{-6} \text{ K}^{-1}$ ; $\alpha_y = 28.3 \times 10^{-6} \text{ K}^{-1}$
Elastic and thermal properties (axial direction) of Dyneema SK65 fibres [45]	$E = 103$ GPa Strength = 3.3 GPa Elongation at break = 3.5% $\alpha = -12 \times 10^{-6} \text{ K}^{-1}$

final thicknesses of unstitched and corresponding stitched panels.

Coupon specimens 20 mm wide, 200 mm long and 1.2 mm thick (Fig. 1b) were cut from the cured panels for static and fatigue tests on an MTS servo-hydraulic machine; all specimens were end-tabbed with fibreglass material to promote gauge length failures. Static testing was performed under stroke control at a rate of 1 mm/min, while fatigue testing was conducted at a stress ratio  $R = 0.1$  using a sinusoidal waveform and a frequency of 2 Hz, which was selected to ensure that the maximum temperature reached by the specimen during the test did not exceed 28 °C. During the tests, the load and strain signals (with strain measured using a 50 mm gauge length extensometer) were continuously acquired to monitor the dynamic stiffness of the sample. The dynamic stiffness was evaluated as the average slope of the stress-strain cycles and proved to be a useful indicator of damage accumulation during fatigue loading.

Images of static and fatigue damage were acquired by penetrant enhanced X-radiography. After interrupting the tests at the prescribed stage of life, the specimens were removed from the testing machine and immersed for 6 h in a Zinc-Iodide solution. The specimens were then cleaned with acetone and exposed to X-ray to reveal nature and extent of the internal damage mechanisms.

### 3. Experimental results and discussion

#### 3.1. Static behaviour

The influence of stitching on the initial stiffness and on the static tensile strength of the laminates is presented in the bar charts of Fig. 2. For each layup, the strength was obtained from tests on at least three specimens, while the stiffness was measured in the strain range from  $0.1 \cdot 10^{-3}$  to  $3.0 \cdot 10^{-3}$  on at least ten specimens, which were subsequently tested in fatigue. It is seen that the insertion of stitches slightly degrades the stiffness of fibre-dominated  $[0/\pm 45/90]_s$  specimens, while it does not affect, within the limits of experimental scatter, the stiffness of matrix-dominated  $[+\theta_2/-\theta_2]_s$  laminates. Small stiffness reductions have been reported in various studies on fibre-dominated composites reinforced by stitches or z-pins [10,28,39,40]; these reductions may be attributed to the typical localized damage features introduced during the stitching process, such as fibre breakage (in the form of clusters of broken fibres at stitch locations) and fibre misalignment or waviness around the stitch thread. The insensitivity of the stiffness of matrix-dominated samples to the presence of stitches can be explained by the

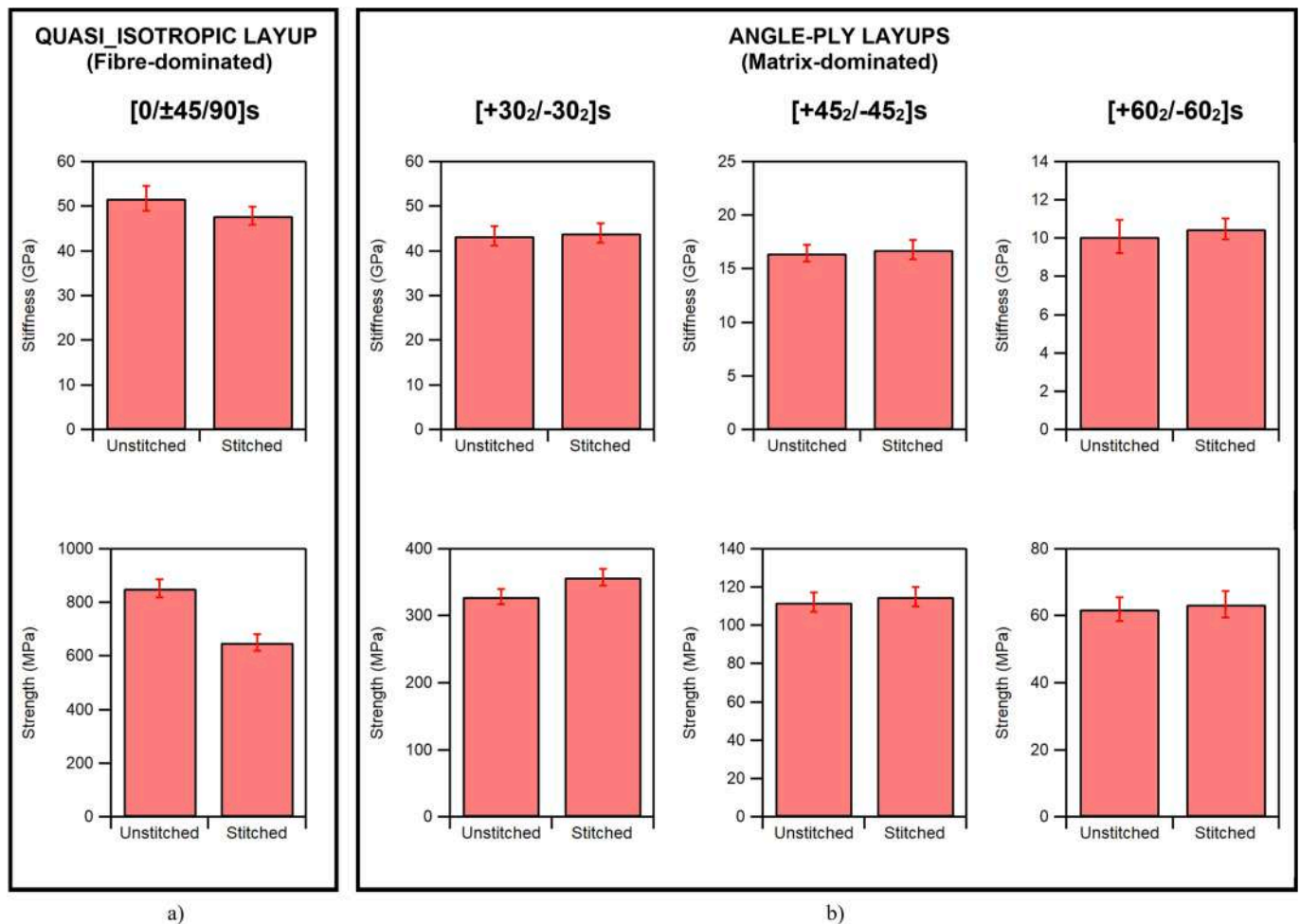


**Fig. 2.** Stiffness (top row) and strength (bottom row) measured under static loading on unstitched and stitched fibre-dominated  $[0/\pm 45/90]_s$  (a) and matrix-dominated  $[+30_2/-30_2]_s$ ,  $[+45_2/-45_2]_s$ ,  $[+60_2/-60_2]_s$  (b) samples.

fact that these manufacturing defects may have a significant effect only in layups with a substantial fraction of layers oriented along the loading direction [39]. The graphs of Fig. 2 show that the effect of stitching on the strength may be adverse or beneficial depending on the stacking sequence. In particular, the introduction of stitches reduces by about 25% the strength of  $[0/\pm 45/90]_s$  laminates but increases by approximately 10% the strength of  $[+30_2/-30_2]_s$  laminates. On the other hand, stitching does not significantly affect the static strength of  $[+45_2/-45_2]_s$  and  $[+60_2/-60_2]_s$  laminates.

Typical tensile stress–strain curves of fibre-dominated  $[0/\pm 45/90]_s$  laminates are illustrated in the graph of Fig. 3 together with X-radiographs of specimens taken close to or after final failure. The stress–strain curves of unstitched samples exhibit a very slight nonlinearity, which may be attributed to delaminations that develop along the edges of the specimen from a stress level of about 50% of the tensile strength. With increasing load, edge delaminations, which mainly affect the  $-45/90$  and  $0/45$  interfaces, propagate toward the axis of the sample, growing up to more than half of the sample width before final failure (see for example the X-radiograph taken at 80% of the failure load). Damage at failure consists of a combination of extensive matrix damage, with widespread delaminations that lead to almost complete separation of various sublaminates, diffuse matrix cracking in  $\pm 45^\circ$  and  $90^\circ$  layers, longitudinal matrix splitting and fibre fracture in load bearing  $0^\circ$  layers.

In stitched  $[0/\pm 45/90]_s$  laminates, in contrast, the growth of delaminations from the edges of the specimen is restrained by the action of stitches, and the main damage modes at failure consist of fibre fractures in association with matrix splitting, which grow in  $0^\circ$  layers from pre-existing defects induced by stitching. The evident stiffness reduction exhibited by stitched quasi-isotropic samples from a stress level of approximately 350 MPa (see the graph of Fig. 3a) corresponds with the onset of these damage modes, which propagate under increasing load up to final failure. The catastrophic failure of the laminate is thought to be initiated when clusters of broken fibres at stitch sites grow to a critical size and trigger the unstable failure of the load-carrying  $0^\circ$  layers along a row of stitches [46]. The change in the damage mechanisms induced by stitching is evident from the radically different fracture appearances of failed unstitched and stitched samples (Fig. 3b). The crucial effect of the clusters of broken fibres generated during the stitching process dominates the failure process of stitched  $[0/\pm 45/90]_s$  laminates and explains their much lower strength in comparison to unstitched laminates.

Fig. 4 shows the stress–strain curves recorded during static tensile

tests on angle-ply samples. We see that  $[+60_2/-60_2]_s$  and, to a smaller degree,  $[+30_2/-30_2]_s$  samples exhibit a rather brittle response in comparison to the  $[+45_2/-45_2]_s$  samples, which have a very ductile behaviour, with a flat stress plateau and large strains at failure. We may also notice that unstitched and stitched laminates with the same layup have similar stress–strain responses, apart from the slight increase in strength after stitching of  $[+30_2/-30_2]_s$  samples. All samples experience a large and sudden drop from the peak load to a much smaller load, which is then sustained upon further straining up to complete separation of the samples in two halves. X-radiographs of angle-ply samples taken immediately after the large load drop and after complete separation are shown in Fig. 5. Unlike quasi-isotropic laminates, stitching does not modify the key damage mechanisms occurring in angle-ply laminates under static loads. The radiographs show that the collapse of all angle-ply layups is fully controlled by matrix damage, with no evidence of broken fibres at the fracture surfaces. In particular, the ultimate failure is triggered by the development of edge to edge  $+ \theta$  matrix cracks, which is followed by visible slippage between the surfaces of the  $+ \theta$  matrix cracks [47] and by the growth of delaminations between the  $+ \theta$  and  $- \theta$  layers. The slightly smaller delaminated area observed just after the load drop in stitched  $[+30_2/-30_2]_s$  and  $[+45_2/-45_2]_s$  laminates in comparison to the unstitched counterparts is due to the restraining effect of stitches on delamination growth. The final damage pattern consists of delaminations bounded by full width  $\pm \theta$  matrix cracks, which cut off the load path and allow the separation of the sample with no fibre fracture. Despite the similar damage mechanisms, the X-ray images show, however, some differences in the evolution and interaction of the damage events leading to the failure of the three angle-ply layups.

In  $[+30_2/-30_2]_s$  laminates (Fig. 5a), damage initiates at the free edge in the form of small triangle-shaped delaminations bounded by short matrix cracks, as a result of the high interlaminar shear stresses generated by the large mismatch in the coefficients of mutual influence between the  $+30^\circ$  and  $-30^\circ$  layers [42]. With increasing load, delaminations form and grow at multiple sites along the sample edges, until major matrix cracks develop on the outer  $+30^\circ$  layers, growing to the entire width of the laminate. Upon the formation of this crack, the load carried by the outer layers is transferred to the inner  $-30^\circ$  layers, thus triggering the immediate development of fine matrix cracking and associated delaminations in a narrow band around the primary  $+30^\circ$  matrix crack. This sudden sequence of damage events induces a dramatic degradation of the structural integrity of the laminate, which

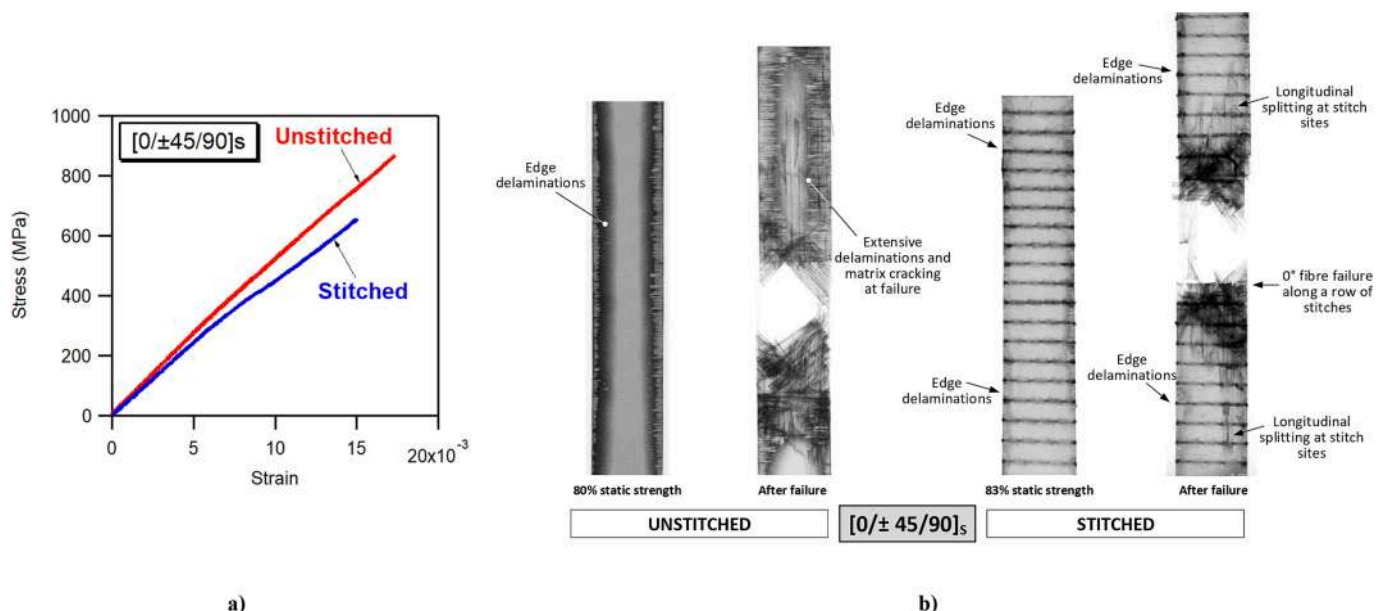


Fig. 3. Typical tensile stress–strain curves (a) and X-radiographs (b) of unstitched and stitched  $[0/\pm 45/90]_s$  samples subjected to static load.

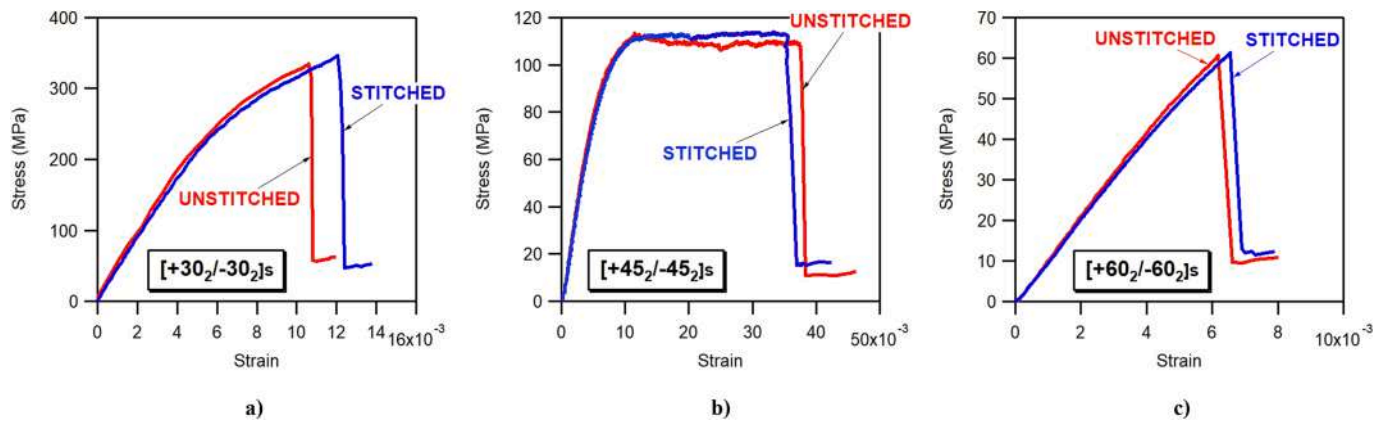


Fig. 4. Typical tensile stress-strain curves of unstitched and stitched  $[+30_2/-30_2]_s$  (a),  $[+45_2/-45_2]_s$  (b) and  $[+60_2/-60_2]_s$  (c) samples subjected to static load.

manifests as the large load drop in the stress–strain curves. As the applied displacement is increased, the highly damaged band across the primary  $+30^\circ$  matrix crack is further strained, leading to the growth of the delaminations over the full width of the laminate up to the final separation of the sample. The comparison of the damage exhibited after failure by the unstitched and stitched  $[+30_2/-30_2]_s$  laminates (Fig. 5a) show that even if stitches, as expected, are not capable of preventing the initiation of edge delaminations, they are effective in restraining their growth. Since the major  $+30^\circ$  matrix cracks that control the final failure of the laminate always originate at the boundary of the most severe edge delamination, the smaller size of edge delaminations in stitched samples plays a beneficial role in delaying the growth of these critical cracks and may account for the higher strength of the stitched samples.

The damage generated by static loads in  $[+45_2/-45_2]_s$  laminates (Fig. 5b) consists of a dense network of fine  $\pm 45^\circ$  matrix cracks that affect the full width and length of the sample, together with some triangle-shaped edge delaminations. Edge delaminations are however much smaller and fewer than those occurring in  $[+30_2/-30_2]_s$  laminates, owing to the much lower interlaminar shear stresses at the free edge of this layup [42]. The sequence leading to ultimate failure is again triggered by the formation of large matrix cracks that grow on the outer  $+45$  layers from an existing edge delamination. However, unlike those in  $[+30_2/-30_2]_s$  laminates, the edge delamination developing in this layup are not sufficiently large to activate the beneficial bridging action of stitches, thus resulting in similar static strength properties of unstitched and stitched laminates.

In  $[+60_2/-60_2]_s$  laminates the ultimate failure is again precipitated by the development of large matrix cracks on the outer layers, but the samples are essentially free of any damage prior to the formation of these critical cracks (Fig. 5c). This damage response is due to the fact that, in this layup, the free edge effects are negligible, and the stress field, and thus the ultimate failure condition, are dominated by the in-plane transverse stress component [42]. The initial damage starts as single matrix cracks in the outer  $+60^\circ$  layers, immediately followed by a sequence of failure events similar to that observed in the other angle-ply layups (i.e., localized shearing of  $-60^\circ$  layers and delamination of the neighbouring  $+60^\circ/-60^\circ$  interfaces), leading first to an immediate drop in load and then to separation of the sample with further applied displacement.

### 3.2. Fatigue behaviour

The fatigue performance of unstitched and stitched fibre-dominated  $[0/\pm 45/90]_s$  laminates is summarized in the S-N graph of Fig. 6, where the maximum applied stress is plotted as a function of the number of cycles to failure. The data show that stitching significantly reduces the fatigue strength of  $[0/\pm 45/90]_s$  specimens, even though the strength degradation generated by stitching decreases with increasing numbers

of cycles, as indicated by the significantly lower slope of the S-logN curve of stitched samples ( $m = -44.9$ ) as compared to that of unstitched samples ( $m = -77.9$ ). Similar fatigue trends were observed in a previous study on quasi-isotropic carbon/epoxy laminates selectively stitched along the free edge [25].

Fig. 7 shows radiographs of damage in  $[0/\pm 45/90]_s$  samples that failed at low (Fig. 7a) and high (Fig. 7b) numbers of cycles. Fig. 7a show samples with short fatigue lives (1205 and 1920 cycles respectively for the unstitched and stitched sample). It must be noted that, despite the comparable fatigue lives, the unstitched sample was subjected to a maximum cyclic stress about 50% higher than that applied to the stitched sample (670 MPa vs 450 MPa). The damage scenario of the unstitched laminate is dominated by matrix damage even for this short fatigue life; matrix cracks and delaminations initiate at the edges since the first cycles and grow continuously during fatigue, with delaminations affecting the entire width of the specimen at failure. As visible in the X-radiograph of Fig. 7a, failed unstitched specimens show extensive delaminations at various interfaces and widespread matrix cracking in the off-axis layers, while fibre failure is only observed in  $0^\circ$  layers in association with longitudinal matrix splitting. In stitched laminates (see Fig. 7a), the propagation of edge delaminations is delayed by the bridging action of stitches, but localized fibre damage and microstructural distortions introduced during the stitching process induce the early development of additional forms of matrix damage such as  $0^\circ$  splitting cracks and associated delaminations at the adjacent  $0^\circ/+45^\circ$  interfaces; these damage mechanisms result in an increase in the load carried by the  $0^\circ$  layers, which accelerates the growth of the clusters of broken fibres and ultimately leads to the final failure of the laminates at a much lower load than the unstitched samples.

A comparison of the typical damage affecting unstitched and stitched samples failed at high numbers of cycles is shown in Fig. 7b. The unstitched and stitched samples were respectively subjected to a maximum stress of 450 MPa and 350 MPa, with corresponding fatigue lives of 347,350 and 494,310 cycles. Under high cycle fatigue, not only unstitched samples but also stitched samples exhibit extensive delaminations, initiated by matrix cracking and splitting at stitch locations. We may argue that for high numbers of cycles the fatigue process of stitched quasi-isotropic laminates is greatly affected by the presence of large delaminations, while the stitching-induced broken fibres play a less critical role than for low numbers of cycles. The delaying effect of stitching on delamination growth may thus partially counteract the adverse effect of the clusters of broken fibres, thus explaining why the degradation of fatigue strength caused by stitching lessens with decreasing stress levels (see the S-N curve of Fig. 6).

The action of different damage mechanisms on the fatigue response of unstitched and stitched  $[0 \pm 45/90]_s$  laminates is also suggested by the different slopes of the S-N curves (Fig. 6) and by the trends of the normalized stiffness (defined as the ratio of the stiffness measured in the

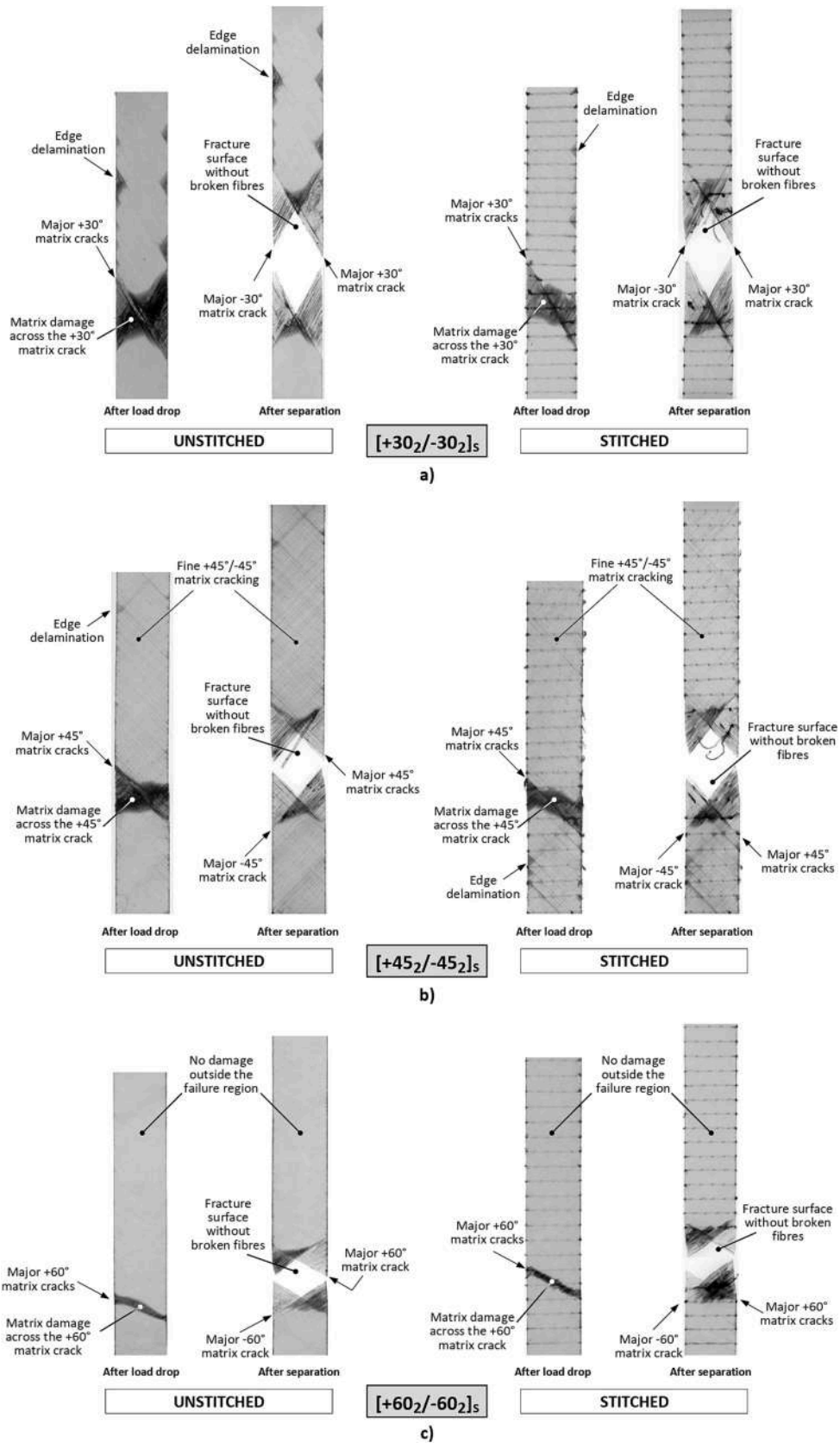


Fig. 5. X-radiographs of unstitched and stitched  $[+30_2/-30_2]_s$  (a),  $[+45_2/-45_2]_s$  (b) and  $[+60_2/-60_2]_s$  (c) samples subjected to static load.

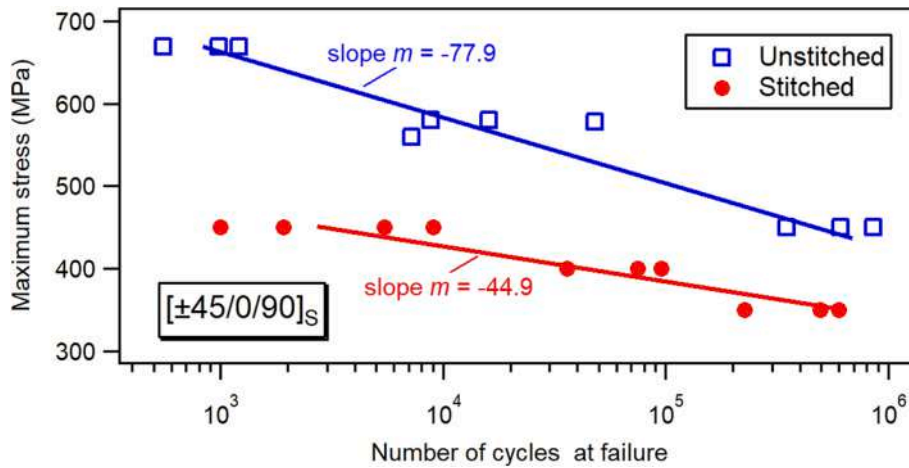


Fig. 6. S-N fatigue data of unstitched and stitched [0/±45/90]s samples.

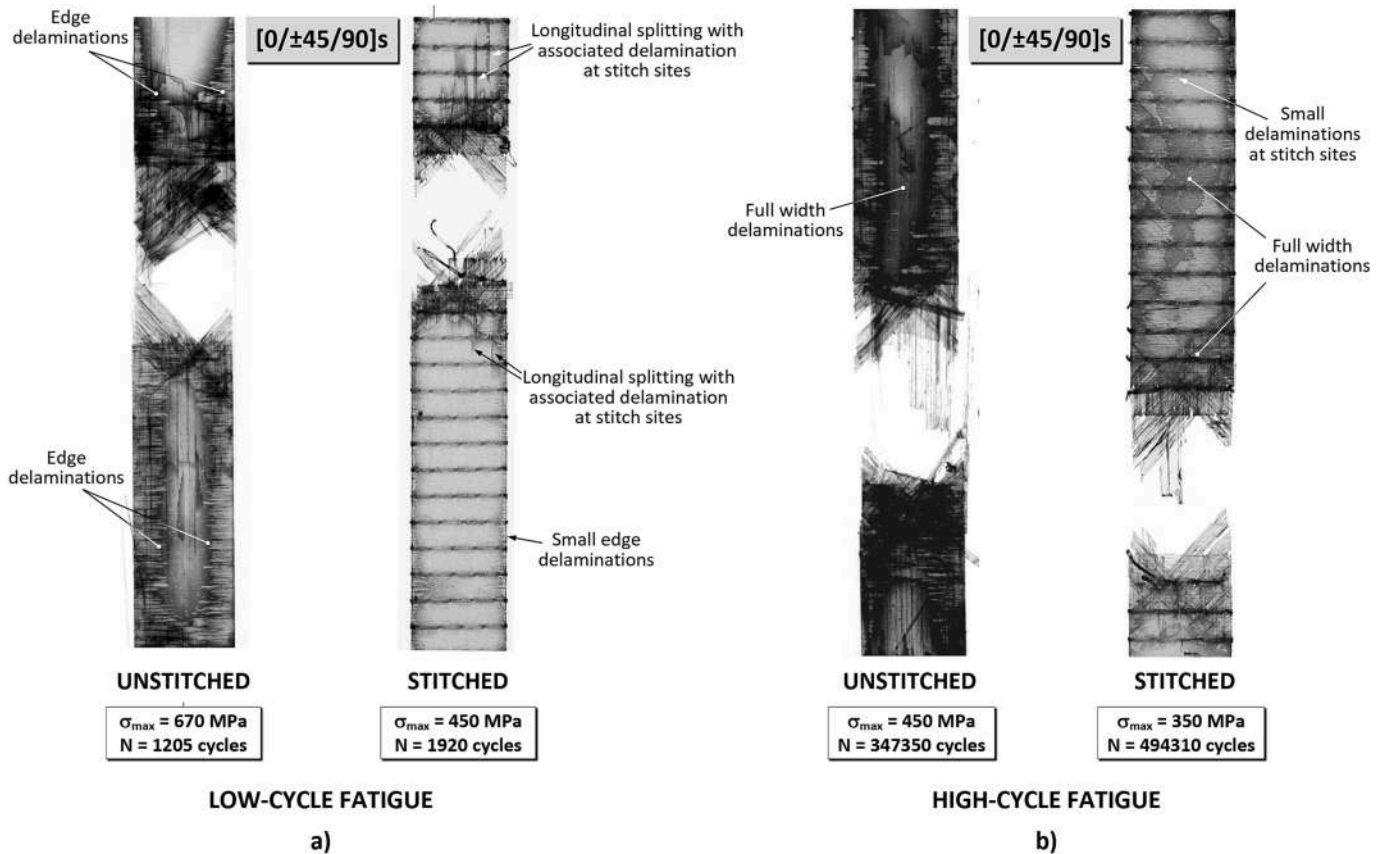
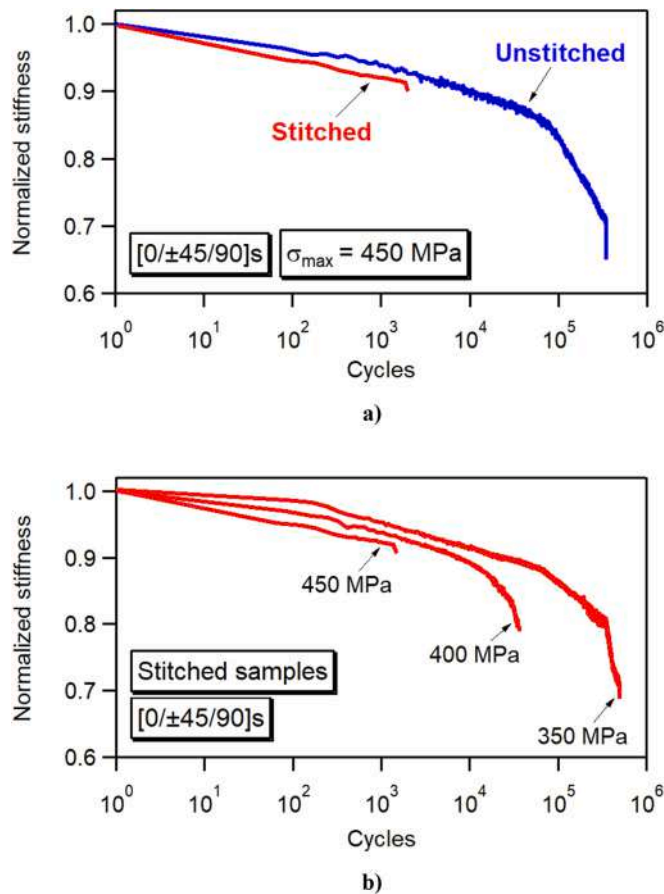


Fig. 7. X-radiographs of unstitched and stitched [0/±45/90]s samples failed under low-cycle (a) and high-cycle (b) fatigue conditions.

current cycle to that measured in the first fatigue cycle) with fatigue cycling (Fig. 8). The graph of Fig. 8a compares the curves of the normalized stiffness measured on unstitched and stitched samples fatigued at the same maximum stress (450 MPa, which corresponds to approximately 50% and 70% of the static strength of unstitched and stitched samples, respectively). Because of the large difference in the number of cycles at failure for the unstitched and stitched samples (respectively 347,350 and 5210 cycles), a logarithmic scale is used on the horizontal axis for an easier comparison of the two histories. We may see that the residual stiffness of the stitched sample immediately before failure is much higher than that of the unstitched sample. This suggests that for low numbers of cycles the fatigue response of the stitched

laminates is dominated by the unstable and fast propagation of localized fibre fracture phenomena, as opposed to the slower and steadier growth of edge delaminations in unstitched laminates. Much larger stiffness drops at failure are however exhibited by stitched samples in the high-cycle fatigue regime (Fig. 8b), because of the higher relative importance of matrix damage mechanisms in the fatigue degradation of the laminate, as seen by comparing the post-failure radiographs of the stitched samples of Fig. 7a (low-cycle fatigue) and Fig. 7b (high-cycle fatigue).

Unlike quasi-isotropic laminates, in which stitching severely degrades both the static and the fatigue performances, the fatigue strength of the angle-ply laminates is enhanced, or at the worst unaffected, by



**Fig. 8.** Evolution of the normalized dynamic stiffness of unstitched and stitched  $[0/\pm 45/90]_s$  samples fatigued at a maximum stress of 450 MPa (a) and of stitched  $[0/\pm 45/90]_s$  samples fatigued at stress levels of 350, 400 and 450 MPa (b).

stitching. As shown by the S-N curves of Fig. 9, while unstitched and stitched  $[+60_2/-60_2]_s$  laminates exhibit similar fatigue lives, the insertion of stitches leads to much better fatigue performances in  $[+30_2/-30_2]_s$  and  $[+45_2/-45_2]_s$  laminates. As an example, the numbers of cycles at failure of stitched  $[+30_2/-30_2]_s$  samples are approximately 2 to 5 times higher than those of the unstitched samples.

X-ray analyses carried out after failure and, for selected samples, at intermediate stages of the fatigue life, indicate that the three angle-ply laminates are affected by similar damage mechanisms and that these mechanisms are not significantly altered by the presence of stitches. The pattern of the fracture surface of unstitched and stitched fatigued samples is analogous to that observed after static failure (see Fig. 10). For all angle-ply layouts, the fracture surface shows extensive delaminations, emanating from the primary  $+\theta$  and  $-\theta$  matrix cracks, which uncouple the  $+\theta$  and  $-\theta$  layers over the full laminate width. No or very little fibre breakage may be observed on the samples after fatigue failure. Even if the three angle-ply layouts exhibit comparable fracture appearances, the relative importance of the damage modes that precede the ultimate failure differs among the three laminates and this explains the different effectiveness of stitches in enhancing their fatigue performance.

The progression of the damage mechanisms leading to the fatigue failure of  $[+30_2/-30_2]_s$  laminates (Fig. 10a) starts with various triangular delaminations that develop at the edges of the samples and grow steadily with fatigue cycling. Edge to edge matrix cracks then develop in the outer  $+30^\circ$  layers from one of the edge delaminations as soon as it reaches a critical size. Finally,  $-30^\circ$  matrix cracks and  $+30^\circ/-30^\circ$  delaminations quickly form and localize in a heavily damaged region around the major  $+30^\circ$  matrix cracks. The damage within this region

propagates very quickly, finally allowing the complete separation of the sample. The increase in fatigue life obtained by stitching, shown by the data reported in the graph of Fig. 9a, may be attributed to the delaying effect of stitches on the growth of edge delaminations. The slower rate of damage propagation in stitched samples is also evident by comparing the decay of stiffness with fatigue cycles in stitched and unstitched samples. Typical examples of histories of stiffness degradation are shown in the graphs of Fig. 11, which present the normalized stiffness vs the number of cycles for unstitched and stitched  $[+30_2/-30_2]_s$  samples subjected to the maximum stress of 240 (Fig. 11a) and 175 MPa (Fig. 11b). We notice that the ultimate fatigue failure of unstitched and stitched samples occurs at approximately the same level of stiffness, and thus at approximately the same degree of damage severity, as also shown by the X-radiographs of damage of Fig. 10a. The curves of Fig. 11 also clearly indicate that damage accumulates at a significantly lower rate in stitched samples. Since the fatigue failure was observed to occur rather quickly after the formation of major matrix cracks on the outer layers, we may reasonably infer that the increase in fatigue life obtained by stitching is mainly due to the restraining effect of stitches on the fatigue growth of the edge delaminations.

The fatigue damage observed after failure in  $[+45_2/-45_2]_s$  samples (Fig. 10b) involves a pattern of fine  $\pm 45^\circ$  matrix cracks and some edge delaminations, although the delaminations are much smaller in size and number than in  $[+30_2/-30_2]_s$  laminates. Failed unstitched and stitched samples are characterized by similar damage severities, as shown by the X-radiographs of Fig. 10b and by the comparable stiffness reductions at failure (Fig. 12). The much slower stiffness degradation exhibited by stitched samples over unstitched samples (Fig. 12) indicates that the improved fatigue life of stitched  $[+45_2/-45_2]_s$  samples is again strictly related to the delaying effect of stitches on the growth of fatigue damage. Examples of fatigue damage progression in unstitched and stitched  $[+45_2/-45_2]_s$  samples are presented in the radiographs of Figs. 13 and 14. We may identify a first phase dominated by diffuse matrix cracking, a second phase where small delaminations form at the edges of the samples, and a final phase where the damage tends first to localize within a heavily strained region emanating from an edge delamination and then to grow up to final failure. We may notice that the largest fraction of fatigue life is spent in the formation and growth of fine and dense matrix cracking, while edge delaminations, which promote the localization of damage at the final separation region, only occur at a very late stage of fatigue lifetime (less than a few percent of the total lifetime in the two samples of Figs. 13 and 14). The experimental observations suggest therefore that under fatigue loads the presence of stitches delays the coalescence and growth of delaminations even for very small crack sizes. This result is somewhat surprising, since the toughening role of stitches is typically observed only when a sufficiently long bridging zone develops behind the crack front [9,12,43,48]. A possible explanation for the beneficial effect induced by stitching may be found in the mechanism of initiation of delamination under mode II loading, which is controlled by the frictional contact generated by shear induced micro cracks at the interfacial resin layer [9]. The distortion and waviness of fibers caused by the stitching process result in an increased friction effect, which may be capable, under cycling loads, of delaying the onset of the interfacial crack and of slowing its growth even for very small crack sizes.

In contrast to  $[+30_2/-30_2]_s$  and  $[+45_2/-45_2]_s$  laminates, the fatigue damage of unstitched and stitched  $[+60_2/-60_2]_s$  laminates consists exclusively of matrix cracks and delaminations that are entirely contained within the fracture region (Fig. 10c). No damage is visible outside the fracture region at any other part of the sample, even for very long fatigue lives. X-ray analyses carried out at different stages of the fatigue history show that the failure initiates directly in the form of  $+60^\circ$  matrix cracks, since no delaminations could be observed at the free edge before fatigue failure. This response is directly related to the internal stress distribution of the  $[+60_2/-60_2]_s$  layout, which is dominated by the intralaminar transverse normal stress, whereas, unlike the other two

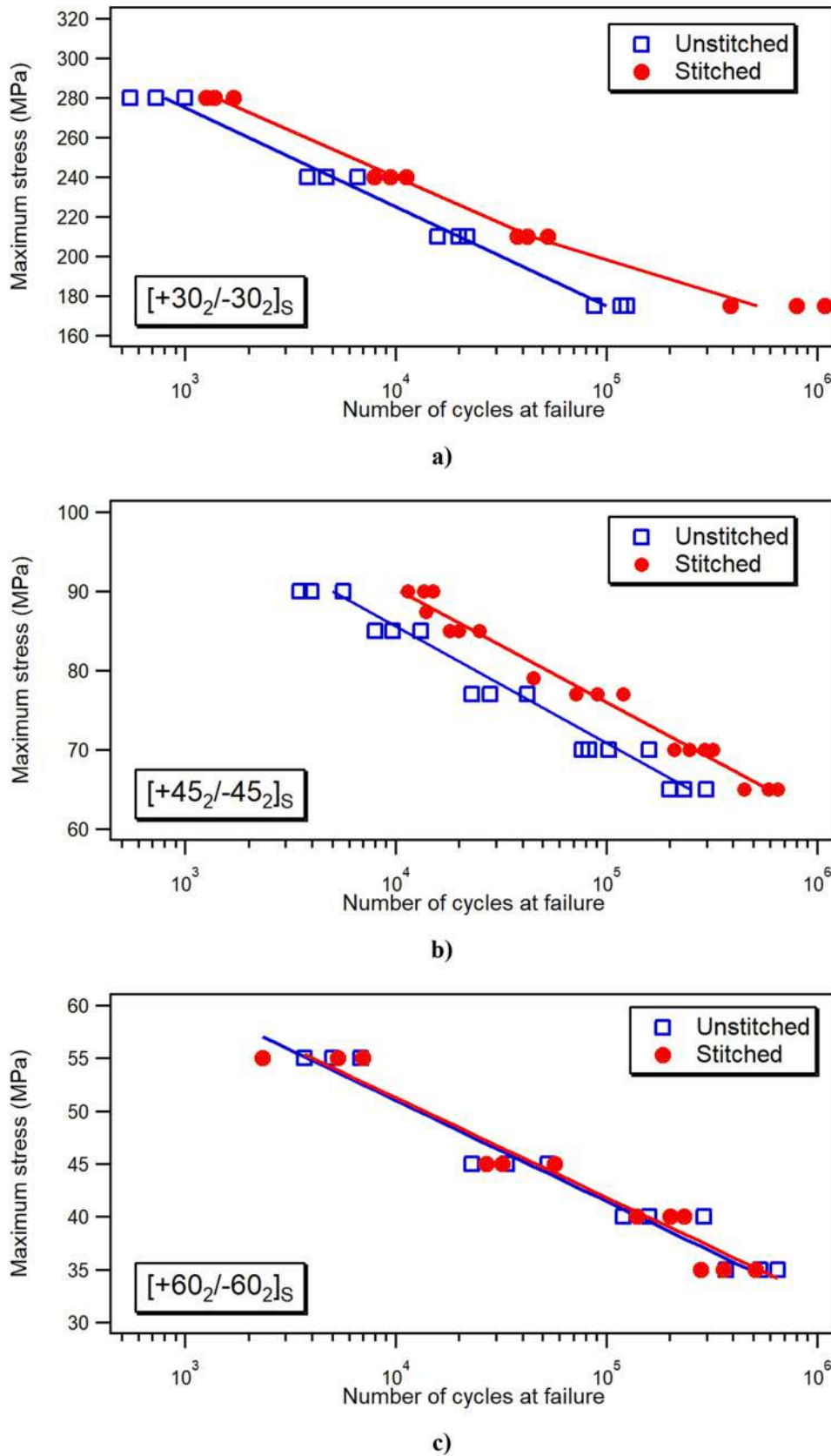


Fig. 9. S-N fatigue data of of unstitched and stitched [+30<sub>2</sub>/-30<sub>2</sub>]<sub>S</sub> (a), [+45<sub>2</sub>/-45<sub>2</sub>]<sub>S</sub> (b) and [+60<sub>2</sub>/-60<sub>2</sub>]<sub>S</sub> (c) samples.

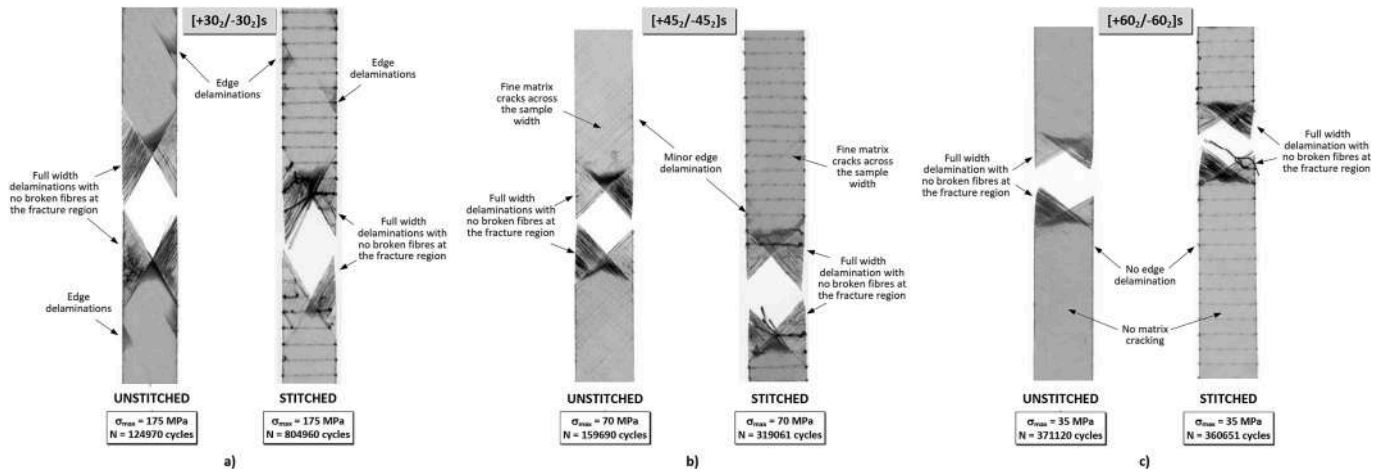


Fig. 10. X-radiographs of unstitched and stitched  $[+30_2/-30_2]_s$  (a),  $[+45_2/-45_2]_s$  (b) and  $[+60_2/-60_2]_s$  (c) samples failed under fatigue loading.

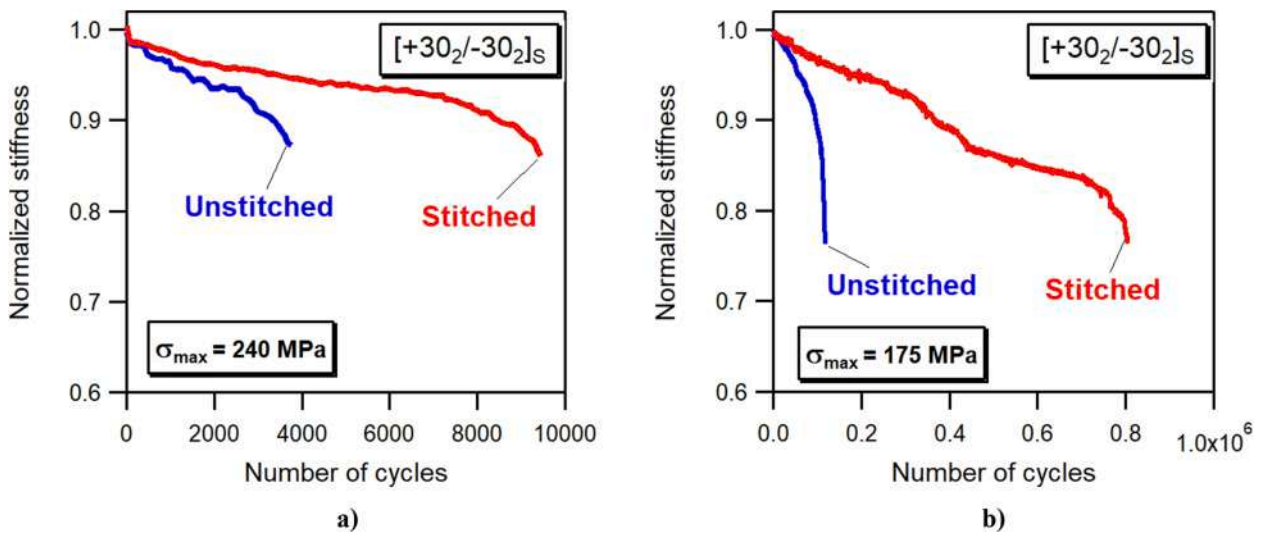


Fig. 11. Evolution of the normalized dynamic stiffness of unstitched and stitched  $[+30_2/-30_2]_s$  samples fatigued at a maximum stress of 240 MPa (a) and 175 MPa (b).

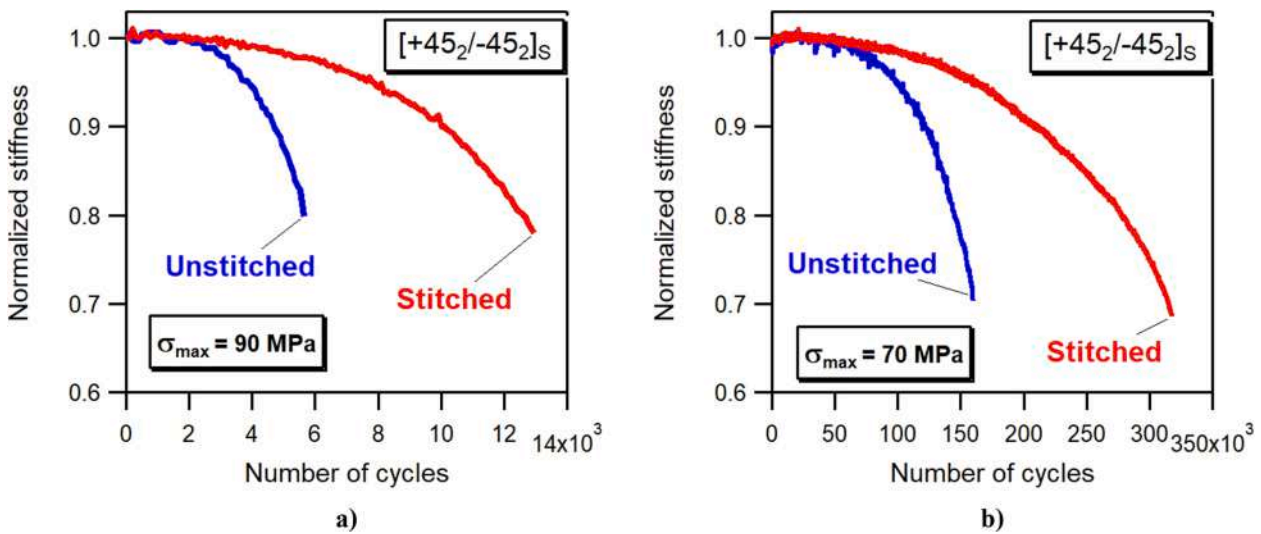


Fig. 12. Evolution of the normalized dynamic stiffness of unstitched and stitched  $[+45_2/-45_2]_s$  samples fatigued at a maximum stress of 90 MPa (a) and 70 MPa (b).

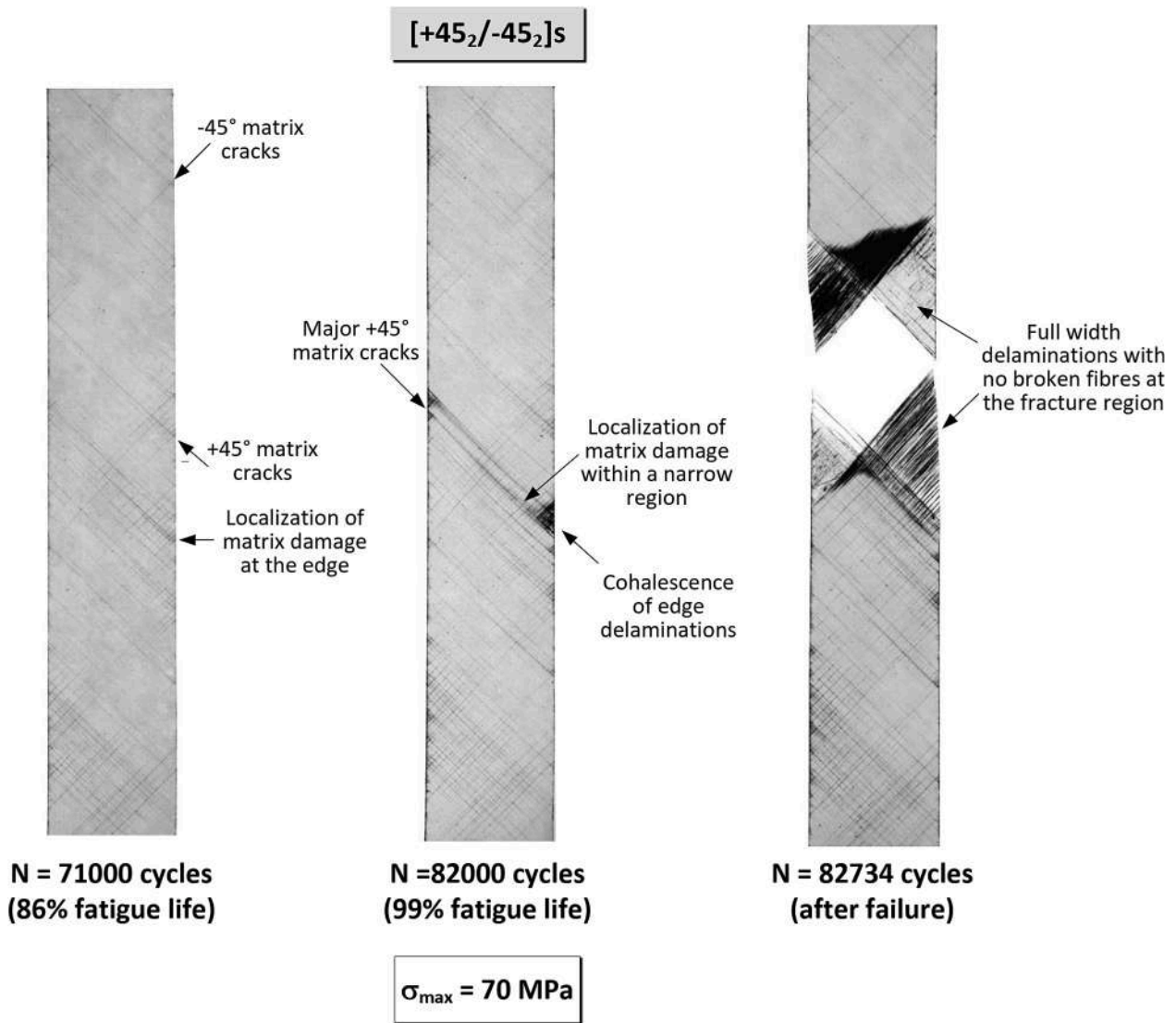


Fig. 13. X-radiographs of fatigue damage evolution in an unstitched  $[+45_2/-45_2]_s$  sample loaded at a maximum stress of 70 MPa.

angle-ply layups, the free edge interlaminar stresses are negligible [42]. A small matrix crack that originates at the free edge is therefore the likely event that triggers the localization of damage and the sudden catastrophic failure. This account of the progression of damage is also supported by the trends of the decrease in stiffness with fatigue cycles (Fig. 15), which show a first stage, spanning over most of the fatigue life, with no substantial stiffness degradation, followed by a final short stage characterized by a rather abrupt stiffness decay and fast failure. This damage scenario, with a rapid failure process essentially triggered by in-plane matrix cracking mechanisms, explains why stitching does not increase the fatigue life of  $[+60_2/-60_2]_s$  laminates, as opposed to  $[+30_2/-30_2]_s$  and  $[+45_2/-45_2]_s$  laminates in which a crucial role is played by edge delaminations over most of the fatigue damage process.

#### 4. Conclusions

Tensile static and fatigue tests were conducted on carbon/epoxy samples with fibre dominated ( $[0/\pm 45/90]_s$ ) and matrix dominated ( $[+30_2/-30_2]_s$ ,  $[+45_2/-45_2]_s$ ,  $[+60_2/-60_2]_s$ ) layups to assess and compare the role of stitching in the mechanical response of laminates with different damage mechanisms and failure modes.

The experimental analyses show that stitching significantly reduces both the static and the fatigue strength of fibre-dominated  $[0/\pm 45/90]_s$

laminates and drastically modifies the damage mechanisms responsible for their final failure. In unstitched laminates, the dominant damage mode preceding the final failure consists of widespread edge delaminations that lead to uncoupling of sublaminates over most of the sample. In stitched laminates the growth of delaminations is restrained by the bridging action of stitches and the key role in the ultimate failure of the sample is played by the unstable propagation of the clusters of broken fibres generated by the stitching process. The adverse effect of stitching on the fatigue strength appears to reduce with decreasing stress levels, as a result of the growing influence of matrix damage mechanisms with increasing numbers of cycles.

With regard to the matrix-dominated angle-ply layups, stitching slightly improves the static strength of  $[+30_2/-30_2]_s$  laminates, while does not affect the static strength of the  $[+45_2/-45_2]_s$  and  $[+60_2/-60_2]_s$  laminates. On the other hand, the introduction of stitches significantly extends the fatigue life of both  $[+30_2/-30_2]_s$  and  $[+45_2/-45_2]_s$  samples but does not modify the fatigue performance of  $[+60_2/-60_2]_s$  samples. The failure of all angle-ply laminates is initiated by the formation of major  $+\theta$  matrix cracks on the outer layers; these cracks trigger the localization of matrix damage on the adjacent  $-\theta$  layers and the fast growth of  $+\theta/-\theta$  delaminations that lead to the separation of the samples in two halves without any fibre fracture. The different effect of stitching on the performance of the three angle-ply layups is related to

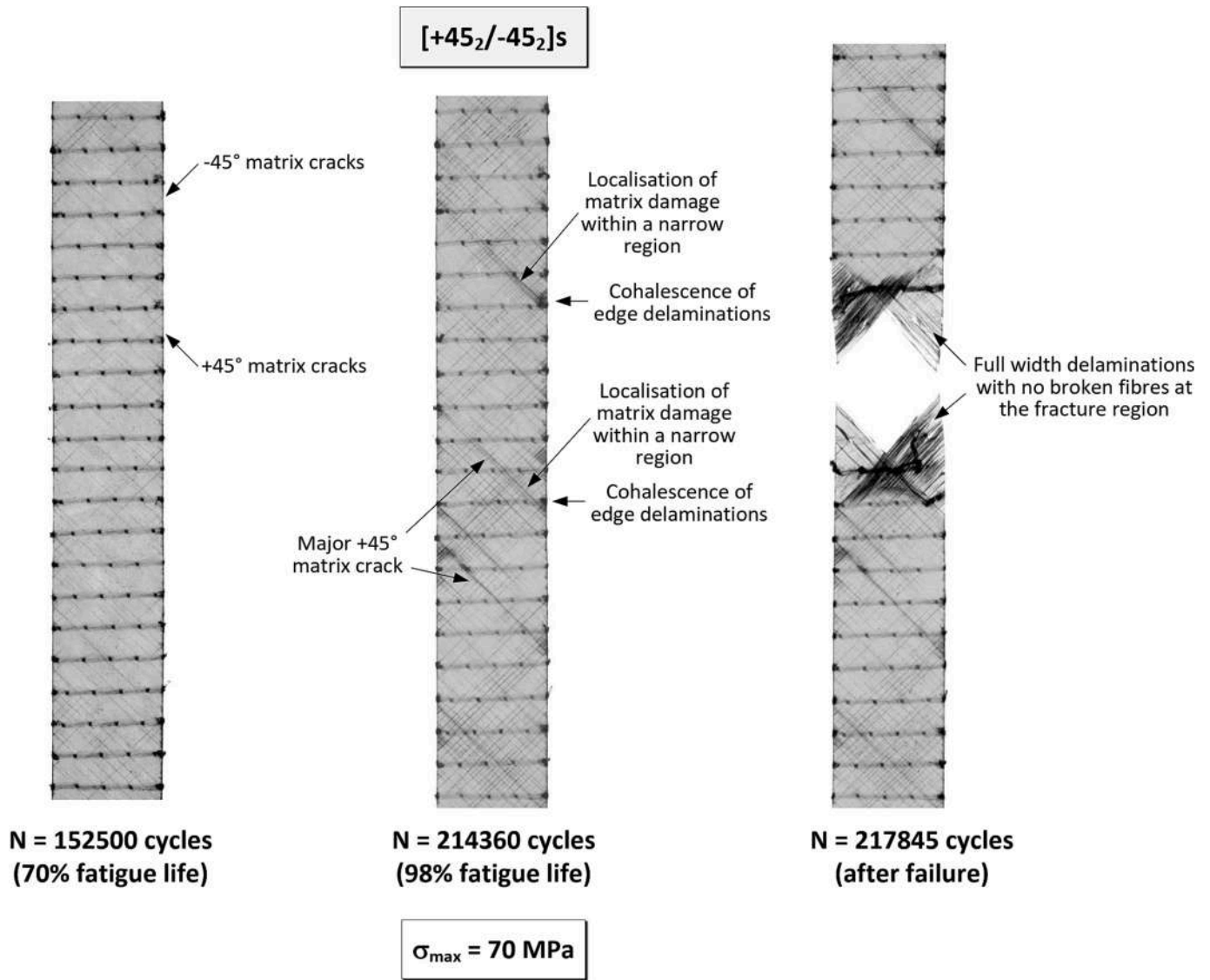


Fig. 14. X-radiographs of fatigue damage evolution in a stitched [+45<sub>2</sub>/-45<sub>2</sub>]s sample loaded at a maximum stress of 70 MPa.

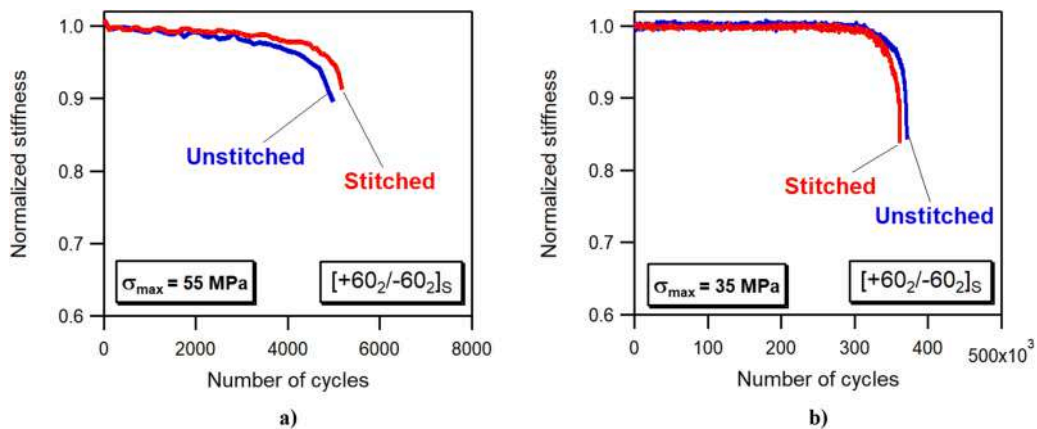


Fig. 15. Evolution of the normalized dynamic stiffness of unstitched and stitched [+60<sub>2</sub>/-60<sub>2</sub>]s samples fatigued at a maximum stress of 55 MPa (a) and 35 MPa (b).

the significance of edge delaminations on the progression of damage up to ultimate failure. In [+30<sub>2</sub>/-30<sub>2</sub>]s and [+45<sub>2</sub>/-45<sub>2</sub>]s laminates, the growth of the critical cracks on the outer + $\theta$  layers is driven by the edge delaminations, and the delaying effect of stitches on the initiation and

growth of free edge delamination accounts for the remarkable improvement in the fatigue strength of these layups. In contrast, the stress distribution in [+60<sub>2</sub>/-60<sub>2</sub>]s laminates is governed by intra-laminar transverse normal stresses and delaminations do not develop

prior to catastrophic failure. Therefore, the potential restraining effect of stitches on delamination growth can not be exploited, resulting in similar strength properties of unstitched and stitched [+60<sub>2</sub>/−60<sub>2</sub>]s samples.

The experimental evidence collected during this study clearly shows that the effectiveness of stitches for enhancing the static and fatigue response of composite laminates greatly depends on the specific layup. The peculiar failure mechanisms that control the damage evolution of the base laminate throughout the entire lifetime should be therefore characterized and understood to evaluate and exploit the potential benefits of the through thickness reinforcements for the considered loading condition.

#### Author contributions

The authors contributed equally to the paper.

#### Declaration of Competing Interest

The authors declare that they have no known competing financial interests or personal relationships that could have appeared to influence the work reported in this paper.

#### Data availability

Data will be made available on request.

#### References

- Wisnom MR. The role of delamination in failure of fibre-reinforced composites. *Philos Trans R Soc A Math Phys Eng Sci* 2012;370:1850–70.
- Kim JK, Mai YW, editors. *Engineered interfaces in fiber reinforced composites*. Oxford: Elsevier; 1998.
- Tong L, Mouritz AP, Bannister MK. *3D fibre reinforced polymer composites*. Oxford: Elsevier; 2002.
- Sridharan S, editor. *Delamination Behaviour of Composites*. Cambridge (UK): Woodhead Publishing Limited; 2008.
- Hoffmann J, Scharr JG. Mechanical properties of composite laminates reinforced with rectangular z-pins in monotonic and cyclic tension. *Compos A Appl Sci Manuf* 2018;109:163–70.
- Cheng C, Chen Z, Huang Z, Zhang C, Tsumi R, Zhou J, et al. Simultaneously improving mode I and mode II fracture toughness of the carbon fiber/epoxy composite laminates via interleaved with uniformly aligned PES fiber webs. *Compos A Appl Sci Manuf* 2020;129:105696.
- Abbasi S, Ladani RB, Wang CH, Mouritz AP. Improving the delamination fatigue resistance of composites by 3D woven metal and composite Z-filaments. *Compos A Appl Sci Manuf* 2021;147:106440.
- Ravindran AR, Ladani RB, Kinloch AJ, Wang C-H, Mouritz AP. Improving the delamination resistance and impact damage tolerance of carbon fibre-epoxy composites using multi-scale fibre toughening. *Compos A Appl Sci Manuf* 2021; 150:106624.
- Mouritz AP, Cox BN. A mechanistic approach to the properties of stitched laminates. *Compos A Appl Sci Manuf* 2000;31(1):1–27.
- Mouritz AP, Cox BN. A mechanistic interpretation of the comparative in-plane mechanical properties of 3D woven, stitched and pinned composites. *Compos A Appl Sci Manuf* 2010;41:709–28.
- Dransfield K, Baillie C, Mai YW. Improving the delamination resistance of CFRP by stitching: a review. *Compos Sci Technol* 1994;50:305–17.
- Jain LK, Dransfield KA, Mai YW. On the effects of stitching in CFRPs—II. Mode II delamination toughness. *Compos Sci Technol* 1998;58:829–37.
- Rys T, Sankar BV, Ifju PG. Investigation of fracture toughness of laminated stitched composites subjected to mixed mode loading. *J Reinf Plast Compos* 2010;29(3): 422–30.
- Sharma SK, Sankar BV. Effect of stitching on impact and interlaminar properties of graphite/epoxy laminates. *J Thermoplast Compos Mater* 1997;10:241–53.
- Tan KT, Watanabe N, Iwahori Y, Ishikawa T. Understanding effectiveness of stitching in suppression of impact damage: An empirical delamination reduction trend for stitched composites. *Compos A Appl Sci Manuf* 2012;43(6):823–32.
- Francesconi L, Aymerich F. Numerical simulation of the effect of stitching on the delamination resistance of laminated composites subjected to low-velocity impact. *Compos Struct* 2017;159:110–20.
- Aymerich F, Priolo P. Characterization of fracture modes in stitched and unstitched cross-ply laminates subjected to low-velocity impact and compression after impact loading. *Int J Impact Eng* 2008;35(7):591–608.
- Tan KT, Watanabe N, Iwahori Y, Ishikawa T. Effect of stitch density and stitch thread thickness on compression after impact strength and response of stitched composites. *Compos Sci Technol* 2012;72(5):587–98.
- Mouritz AP, Leong KH, Herszberg I. A review of the effect of stitching on the in-plane mechanical properties of fibre-reinforced polymer composites. *Compos A Appl Sci Manuf* 1997;28(12):979–91.
- Farley GL, Dickinson LC. Removal of surface loop from stitched composites can improve compression and compression-after impact strengths. *J Reinf Plast Compos* 1992;11(6):633–42.
- Vandermeij NE, Masters JE, Poe CC, Morris DH. Compression-compression fatigue of a stitched uniwoven graphite/epoxy composite. *ASTM Spec Tech Publ* 1994; 1185:258.
- Reeder JR. Stitching vs. a toughened matrix: compression strength effects. *J Compos Mater* 1995;29(18):2464–87.
- Kang TJ, Lee SH. Effect of stitching on the mechanical and impact properties of woven laminate composite. *J Compos Mater* 1994;28:1574–87.
- Shah Khan MZ, Mouritz AP. Fatigue behaviour of stitched GRP laminates. *Compos Sci Technol* 1996;56:695–701.
- Mouritz AP, Priolo P, Sun CT. Static and fatigue behaviour of stitched graphite/epoxy composite laminates. *Compos Sci Technol* 2003;63(6):907–17.
- Mouritz AP. Fracture and tensile fatigue properties of stitched fibreglass composites. *Proc Inst Mech Engineers, Part L: J Mater Design Appl* 2004;218(2): 87–93.
- Rudov-Clark S, Mouritz AP. Tensile fatigue properties of a 3D orthogonal woven composite. *Compos A Appl Sci Manuf* 2008;39:1018–24.
- Yudhanto A, Lubineau G, Ventura IA, Watanabe N, Iwahori Y, Hoshi H. Damage characteristics in 3D stitched composites with various stitch parameters under in-plane tension. *Compos A Appl Sci Manuf* 2015;71:17–31.
- Lubowski SJ, Poe CC. Fatigue characterization of stitched carbon/epoxy composites. In: *Proceedings of Fiber-Tex 1987 conference*; 1987. p. 253–71.
- Dow MB, Smith DL. Damage-tolerant composite materials produced by stitching carbon fabrics. In: *Proceedings of the 21st International SAMPE Technical Conference*; 1989. p. 595–605.
- Portanova M, Poe C, Whitcomb J. Open hole and postimpact compressive fatigue of stitched and unstitched carbon-epoxy composites. In: *Grimes GC, editor. Composite materials: Testing and design (Tenth Volume)*, ASTM STP 1120. Philadelphia: American Society for Testing and Materials; 1992. p. 37–53.
- Furrow KW, Loos AC, Cano RJ. Environmental effects on stitched RTM textile composites. *J Reinf Plast Compos* 1996;15(4):378–419.
- Herszberg I, Loh A, Bannister MK, Thuis HGJSJ. Open hole fatigue of stitched and unstitched carbon/epoxy laminates. In: *Proceedings of ICCM-11 (Volume V)*, Gold Coast, Australia, July 1997, pp.138–148.
- Sun CT, Mignery LA, Jih CJ. A study of stitching as a thickness directional reinforcement in graphite/epoxy laminates [CML 84-10 report]. Purdue University: Composite Materials Lab, School of Aeronautics and Astronautics, 1984.
- Huang T, Jiao G, Zhao L. Fatigue Behavior of Stitched Carbon/Bismaleimide Composite Laminates. *J Reinf Plast Compos* 2007;26(3):297–303.
- Beier U, Wolff-Fabris F, Fischer F, Sandler JKW, Altstädt V, Hülster G, et al. Mechanical performance of carbon fibre-reinforced composites based on preforms stitched with innovative low-melting temperature and matrix soluble thermoplastic yarns. *Compos A Appl Sci Manuf* 2008;39:1572–81.
- Carvelli V, Tomaselli VN, Lomov SV, Verpoest I, Witzel V, Broucke BVD. Fatigue and post-fatigue tensile behaviour of non-crimp stitched and unstitched carbon/epoxy composites. *Compos Sci Technol* 2010;70(15):2216–24.
- Yudhanto A, Watanabe N, Iwahori Y, Hoshi H. Effect of stitch density on fatigue characteristics and damage mechanisms of stitched carbon/epoxy composites. *Compos A Appl Sci Manuf* 2014;60:52–65.
- Mouritz AP. Tensile fatigue properties of 3D composites with through-thickness reinforcement. *Compos Sci Technol* 2008;68(12):2503–10.
- Mouritz AP, Chang P. Tension fatigue of fibre-dominated and matrix-dominated laminates reinforced with z-pins. *Int J Fatigue* 2010;32(4):650–8.
- Piggott MR. Structural design with angle ply laminates - Why and how. *Adv Compos Lett* 2004;13(1):71–5.
- Herakovich CT. *Failure and Damage (Chapter 9)*. In: *Mechanics of Fibrous Composites, Chapter 9: Failure and Damage* New York, Wiley, 1998. p. 303–61.
- Drake DA, Sullivan RW, Lovejoy AE, Clay SB, Jegley DC. Influence of stitching on the out-of-plane behavior of composite materials—A mechanistic review. *J Compos Mater* 2021;55(23):3307–21.
- Pieczonka L, Aymerich F, Brozek G, Szewdo M, Staszewski WJ, Uhl T. Modelling and numerical simulations of vibrothermography for impact damage detection in composites structures. *Struct Control Health Monit* 2013;20:626–38.
- Fibrxl – Dyneema Product Data Sheet – FXL 07 – 2020. <https://fibrxl.com/wp-content/uploads/2020/07/FibrXL-PDS-performance-0720-DEF-Dyneema.pdf> (accessed February 26, 2023).
- Chang P, Mouritz AP, Cox BN. Properties and failure mechanisms of z-pinned laminates in monotonic and cyclic tension. *Compos A Appl Sci Manuf* 2006;37(10): 1501–13.
- Saleh MN, Yudhanto A, Potluri P, Lubineau G, Soutis C. Characterising the loading direction sensitivity of 3D woven composites: Effect of z-binder architecture. *Compos A Appl Sci Manuf* 2016;90:577–88.
- Sankar BV, Sharma SK. Mode II delamination toughness of stitched graphite/epoxy textile composites. *Compos Sci Technol* 1997;57(7):729–37.